NANOSYSTEMS: PHYSICS, CHEMISTRY, MATHEMATICS, 2017, 8 (4), P. 462–470

Synthesis of CaF_2–YF_3 nanopowders by co-precipitation from aqueos solutions

P. P. Fedorov[1], M. N. Mayakova[1], S. V. Kuznetsov[1], V. V. Voronov[1], Yu. A. Ermakova[1], A. E. Baranchikov[2]

[1]A. M. Prokhorov General Physics Institute, Russian Academy of Sciences
38 Vavilov Street, Moscow, 119991, Russia

[2]N. S. Kurnakov Institute of General and Inorganic Chemistry,
Russian Academy of Sciences, Leninskii pr. 31, Moscow, 119991, Russia

ppfedorov@yandex.ru

DOI 10.17586/2220-8054-2017-8-4-462-470

Study of the CaF_2–YF_3 system by co-precipitation from aqueous nitrate solutions revealed the formation of $Ca_{1-x}Y_xF_{2+x}$ solid solution precipitate containing up to 20 mol. % yttrium fluoride ($x \leq 0.2$). A higher yttrium to calcium ratio in the starting solutions caused additional precipitation of orthorhombic β-YF_3 nanophase elongated along the $\langle b \rangle$ axis. Cubic $(H_3O)Y_3F_{10}$ phase was also formed (SSG *Fm3m*, a = 11.60 Å, KY_3F_{10} structural type).

Keywords: calcium fluoride, yttrium fluoride, nanopowders.

Received: 19 July 2017

Revised: 2 August 2017

1. Introduction

The CaF_2–YF_3 system, along with the NaF–YF_3 system [1–4], plays a particularly important role among binary fluoride systems. Solid solution of yttrium fluoride in calcium fluoride is a classic example of heterovalent isomorphism [5]. Its study was initially discussed by Vogt in treatises on yttrofluorite [6], and has continued for more than a hundred years [7–24] (for a more detailed history of this study, please see [18]): the said CaF_2–YF_3 system has become a model for describing the interaction of calcium fluoride with the rare earth fluorides from yttrium group of elements (see Fig. 1). The CaF_2–YF_3 system is also the basis for several natural fluoride minerals [6, 15, 25–27].

Yttrium cation substitutes calcium ions in the fluorite structure, and supplementary fluoride anions, penetrating the formed crystal lattice, compensate for the corresponding changes in electrostatic charges for the sake of electrical neutrality of the system. The formed cationic and anionic defects associate among themselves, thus forming defect clusters [28, 29]. $Ca_{1-x}Y_xF_{2+x}$ solid solution maintains its original fluorite-type structure within the $0 \leq x \leq 0.38$ interval limits. A smooth maximum in the melting curves of $Ca_{1-x}Y_xF_{2+x}$ at x = 0.11 (Fig. 1) allows the growth of high-quality $Ca_{1-x}Y_xF_{2+x}$ single crystals from its melts with $x \leq 0.15$.

Such synthetic $Ca_{1-x}Y_xF_{2+x}$ yttrofluorite crystals have become widely used photonics materials, including solid state laser matrices [13]. Also, introducing yttrium fluoride into the calcium fluoride crystal lattice causes dramatic changes in its physical properties, including fluoride-ion ionic conductivity, hardness, cleavage and heat conductivity (the latter two parameters decrease significantly) [23, 30]. Relatively high yttrium concentrations complicate $Ca_{1-x}Y_xF_{2+x}$ single crystal growth from the melts due its incongruent melting, and the formation of a cellular substructure [31, 32], and local ordering of the formed solid solution [7, 12]. Additional increase in the YF_3 content in the CaF_2–YF_3 system leads to the formation of another berthollide-type variable-composition solid solution at 65–75 mol. % YF_3 with hexagonal LaF_3 tysonite-type structure [10, 11]. This phase undergoes metastable ordering under cooling. Another solid solution, based on high-temperature α-YF_3 polymorph, is also formed in the CaF_2-YF_3 system [33].

Fedorov [21] reported the lower temperature part of the phase diagram of the CaF_2–YF_3 system, taking into account the results for Kuntz's [15] hydrothermal studies and Bergstol et al. [25] investigation of tveitite mineral formation under natural conditions (tveitite is an ordered fluorite-type phase), and considering that fluorite-type solid solutions undergo ordering with the formation of a series of fluorite-type phases when cooled [4,12]. The latter fluorite-type phases contain Y_6F_{37} clusters in their crystal lattices with Thompson antiprism coordination yttrium polyhedra. Such clusters fit in naturally in the fluorite crystal lattice (Fig. 2) and appear to be the dominant type of structural defects in $Ca_{1-x}Y_xF_{2+x}$ solid solutions at higher yttrium concentrations [14, 16, 28, 29]. The heterovalent substitution mechanism for the formation of the aforementioned solid solutions (Fig. 2) can be described by the following equation:

$$(M_6F_{32})^{20-} \rightarrow (Y_6F_{37})^{19-} + F^-_{int}. \quad (1)$$

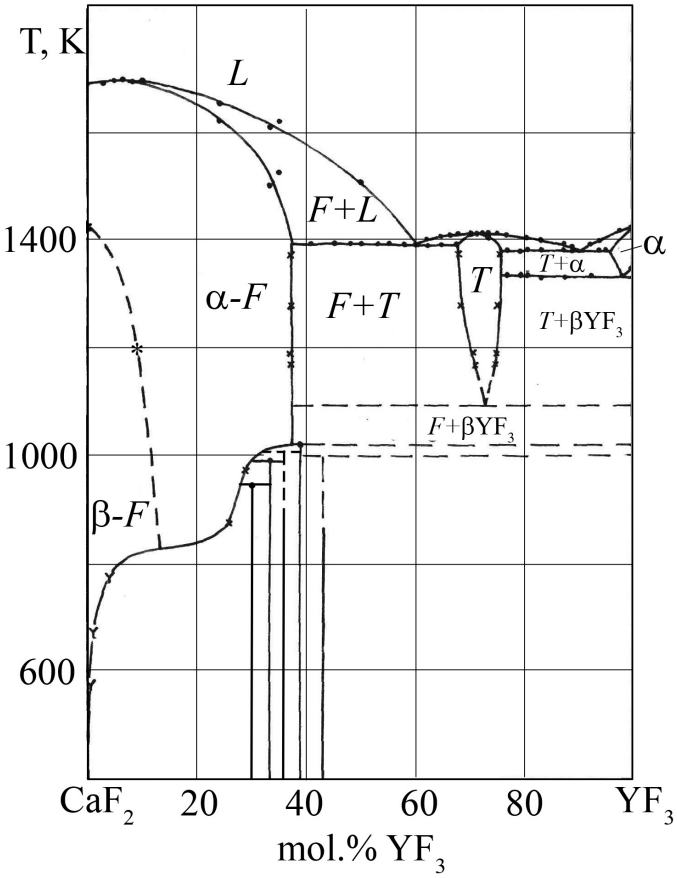

FIG. 1. Phase diagram of the CaF_2–YF_3 system [17]. L – melt, F –$Ca_{1-x}Y_xF_{2+x}$ fluorite-type solid solution, T – tysonite (LaF_3) type berthollide phase

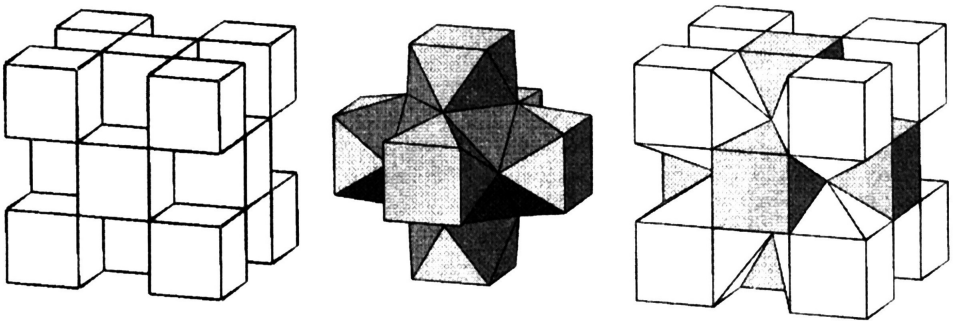

FIG. 2. Insertion of R_6F_{37} clusters into the fluorite matrix

Nanofluorides are another rapidly developing area of the modern science [34–39], for nanofluorides are widely implemented as luminophores, catalysts, biomedical and electrochemical materials; the CaF_2–YF_3 system has also become crucially important in this area, as well. Low-temperature and soft chemistry syntheses of nanofluorides (e.g, mechanochemical [40, 41], sol-gel [24], solvothermal [42] methods and some other techniques [35]) are especially prominent because of their technological advantages. Recently, we have successfully used our co-precipitation from aqueous solutions methods for nanofluoride preparations [34,35,43–48], including our systematic studies of phase formations in the BaF_2–YF_3 [49], BaF_2–BiF_3 [50], BaF_2–ScF_3 [51], BaF_2–CeF_3 [52], SrF_2–YF_3 [53] and CaF_2–HoF_3 [54] systems. We have observed varieties of phase fields in the studied MF_2–YF_3 and NaF–RF_3 systems, including non-equilibrium phases with wide areas of homogeneity; we have also observed the absence of the ordered phases that exist under higher temperature equilibrium conditions [4].

Thus, according to the background given above, the purpose of the present study was the investigation of nanophase formation in the CaF_2–YF_3 system under co-precipitation from aqueous solutions at lower temperatures.

2. Experimental

We used 99.99 wt.% pure $Y(NO_3)_3{\cdot}6H_2O$ and $Ca(NO_3)_2{\cdot}4H_2O$ (manufactured by OOO Lanchit), as well as 99.9 % pure 40 wt.% aqueous HF (manufactured by TECH System) and double distilled water as starting materials without any further purification.

Specimens in the CaF_2–YF_3 system were prepared by co-precipitation from aqueous solutions in polypropylene reactors according to previously-described procedures [4, 49, 53, 54]. 0.2 Mol/L aqueous nitrate solutions in double distilled water were vigorously mixed with magnetic stirring bar and then added dropwise under continued stirring to a 2-fold excess of 5 vol.% aqueous HF. The formed precipitates were decanted, rinsed with double distilled water until a pH of 5–6 was obtained. In some experiments, precipitates were additionally neutralized with aqueous ammonia (99.9 % pure) and then rinsed again with double distilled water until a pH of 5–6 was maintained. All precipitates were air-dried at 40 °C.

Phase composition of the synthesized samples was characterized by X-ray powder diffraction (Bruker D8 diffractometer; CuK_α radiation; TOPAS software package for experimental data treatment and coherent scattering domain and microdeformation size calculations). Particle dispersity and morphology were controlled by scanning electron microscopy (SEM) (NVision 40 microscope). The same NVision 40 microscope was also used for the sample chemical analyses (X-ray spectroscopy). Specimen chemical composition was also studied by atomic emission spectroscopy (AES) with the use of LEA-S500 analyzer (OOO SOL Instruments, Minsk, Belarus) (see Supporting Information for the further details). MOM Q-1500D PaulikPaulikErdey derivatograph has been utilized for the thermal analysis investigations (Pt crucibles, air).

3. Results and Discussion

Colloid solutions in the CaF_2–YF_3 system were obtained during the synthesis in which the precipitate formed very slowly (couple of weeks) (Figs. 3–7; Tables 1, 2). SEM data (Fig. 3) confirmed that the precipitated nanoparticles were actually of the small sizes. Chemical analyses of both types, X-ray spectroscopy and AES (Table 1, also see Supplemental Information), have shown that the metal ratios in the formed solid precipitates were close to the corresponding ratios in the starting aqueous solutions/mixtures even if the observed ratio differences were a little bit larger than in the case of the previously studied SrF_2–YF_3 [53] and BaF_2–YF_3 [49] systems.

X-Ray diffraction data indicated that precipitates formed from solutions with 20 mol. % YF_3 or less were CaF_2-based fluorite-type solid solutions (cubic system, $Fm3m$ SSG). SEM image of the 10 mol. % YF_3 specimen (i.e., precipitated from the 10 % Y^{3+} and 90 % Ca^{2+} solution) contained readily-visible/resolved agglomerates of the same phase particles 30–50 nm in diameter. Experimental data for the unit lattice parameters of precipitated $Ca_{1-x}Y_xF_{2+x}$ solid solutions coincided within the 0.004 Å range with the a(x) concentration dependency function for $Ca_{1-x}Y_xF_{2+x}$ solid solutions, synthesized at higher temperatures [55] (Fig. 7). However, in addition to the increasing crystal lattice parameter, X-ray diffraction patterns of precipitates $Ca_{1-x}Y_xF_{2+x}$ contained weak (200) lines at about 32.5 ° 2θ (this line is absent in the X-ray diffraction pattern of the pure face-centered CaF_2). The latter observation was an additional evidence of the solid solution formation.

X-Ray diffraction patterns of $Ca_{1-x}Y_xF_{2+x}$ samples with 30 mol. % or more YF_3 contained broadened lines of β-YF_3 nanoparticles (orthorhombic system, *Pnma* SSG [18]) (Figs. 4–5). However, relative clarity of (020) β-YF_3 line at about 26 ° 2θ indicated that crystal lattices of the said β-YF_3 nanoparticles were stretched along $\langle b \rangle$ axis.

All precipitated fluorides were hydrated and contained about 5.5 ± 0.3 wt. % water (DTA data, see Supplemental Information). Heating of these specimens was accompanied with mass losses that continued to 450–500 °C. X-Ray diffraction patterns of such samples annealed at 450–500 °C contained only narrowed lines, and the latter phenomenon was an unequivocal evidence of the nanoparticle enlargement.

Synthesis of the 90 % YF_3 – 10 % CaF_2 solid solution resulted in the formation of the novel phase (Fig. 4) with the X-ray diffraction pattern indexed in the P-cubic system with a = 5.800(2) Å parameter (Table 2) or in the F-cubic system with a = 11.60 Å (calculated size of the coherent scattering domain D = 25 nm). The SEM image of this specimen contained joined together plate-type nanocrystals (Figs. 3c and 3d).

The X-Ray diffraction pattern of this phase was similar to the one of KY_3F_{10} (*Fm3m* SSG, Z = 8), so one could assume that it was $(H_3O)Y_3F_{10}$ compound with hydroxonium ions occupying potassium sites in the crystal lattice. Heating the specimen resulted in about 11.3 wt. % mass loss (Supplemental Information), which might

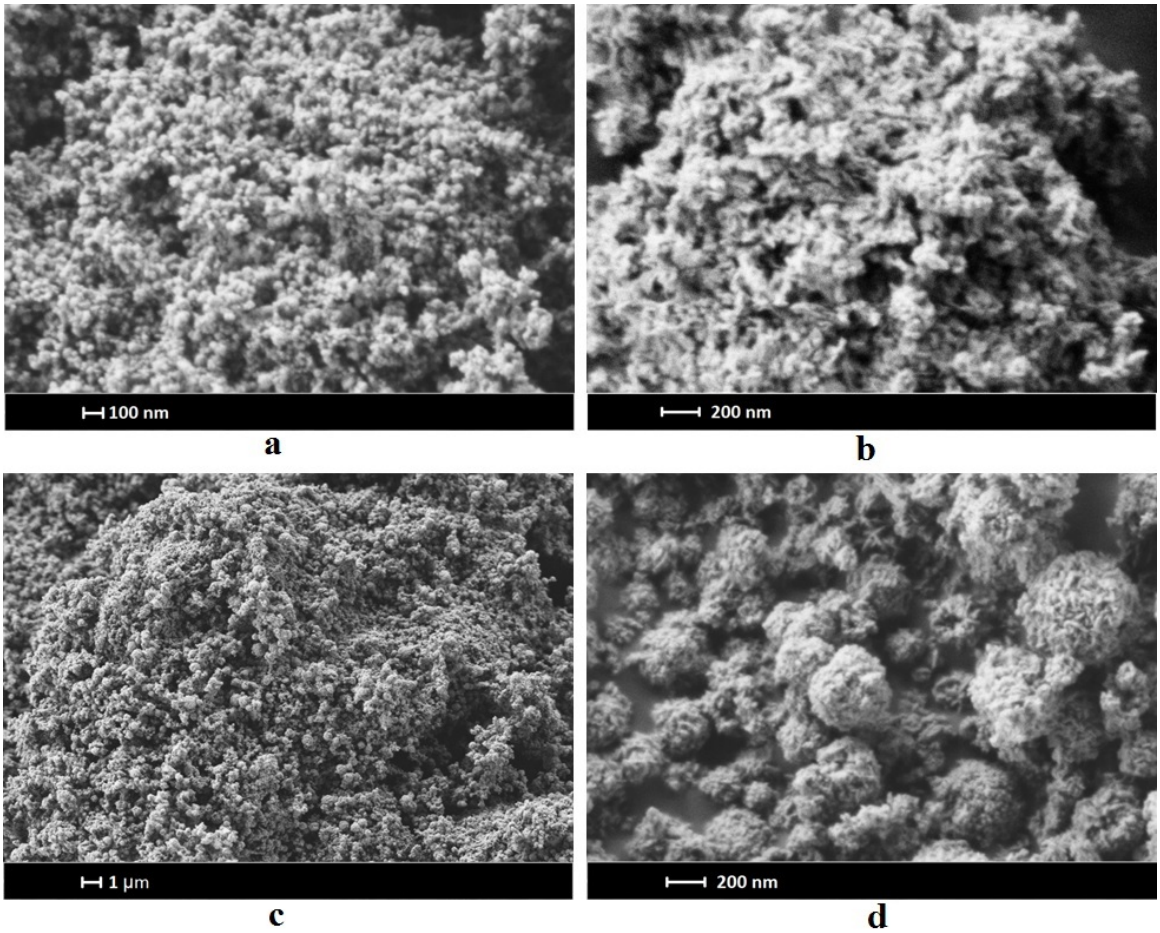

FIG. 3. SEM images of the CaF_2-YF_3 specimens: 10 mol. % YF_3 (a), 50 % mol. YF_3 (b), 90 % mol.% YF_3 (c, d)

TABLE 1. Chemical analysis of CaF_2–YF_3 specimens

Sample composition	Refined YF_3 content, mol. %		
	X-Ray spectroscopy (electron microscopy)	Atomic emission spectroscopy (AES)	
		290 nm excitation wavelength	320 nm excitation wavelength
$Ca_{0.70}Y_{0.30}F_{2.30}$ (30.0 mol. % YF_3)	–	26.06±0.75	25.85±0.92
$Ca_{0.50}Y_{0.50}F_{2.50}$ (50.0 mol. % YF_3)	52.4	52.01±1.69	54.14±1.85
$Ca_{0.30}Y_{0.70}F_{2.70}$ (70.0 mol. % YF_3)	–	68.83±2.16	73.31±1.41
$Ca_{0.10}Y_{0.90}F_{2.90}$ (90.0 mol. % YF_3)	90.8	–	–

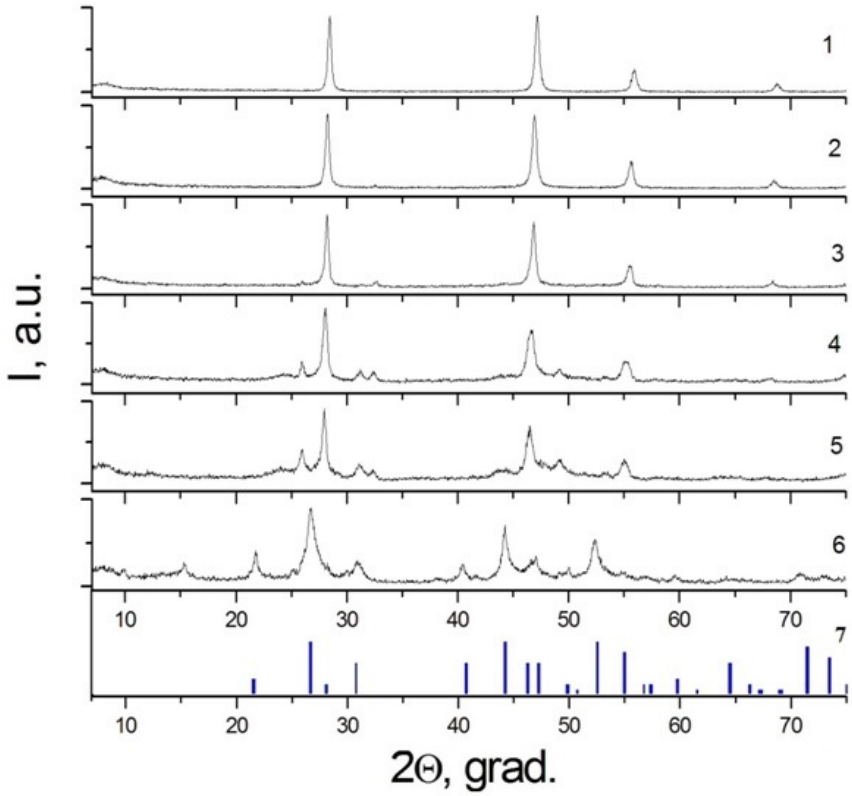

FIG. 4. X-Ray powder diffraction patterns for the specimens obtained by co-precipitation of calcium and yttrium fluorides from aqueous nitrate solutions: 10 mol.% (1); 20 mol.% (2); 30 mol.% (3); 50 mol.% (4); 70 mol.% (5); 90 mol.% (6) YF_3 (nominal compositions), and JCPDS Card No. 27-0465 for KY_3F_{10} phase (7)

TABLE 2. X-Ray diffraction pattern of the $Ca_{0.10}Y_{0.90}F_{2.90}$ specimen ($Q = 10^4/d^2$. P-cubic lattice, $a = 5.800(2)$ Å, $F(14) = 11.9$, $M(14) = 25.8$)

N	$2O$(obs)	d(obs), Å	Q(obs)	I/I_0,%	h k l	Q(calc)	ΔQ
1	15.320	5.7789	299.44	15	1 0 0	297.25	2.19
2	21.730	4.0866	598.79	39	1 1 0	594.50	4.29
3	26.740	3.3312	901.15	100	1 1 1	891.75	9.40
4	30.900	2.8915	1196.06	15	2 0 0	1189.00	7.06
5	38.020	2.3648	1788.18	5	2 1 1	1783.50	4.68
6	44.240	2.0457	2389.55	75	2 2 0	2378.00	11.55
7	47.000	1.9318	2679.64	30	2 2 1	2675.25	4.38
8	52.350	1.7463	3279.16	50	3 1 1	3269.75	9.40
9	54.740	1.6755	3562.14	10	2 2 2	3567.00	−4.86
10	59.530	1.5516	4153.75	7	3 2 1	4161.50	−7.75
11	64.170	1.4502	4754.93	3	4 0 0	4756.01	−1.07
12	70.820	1.3294	5658.34	8	3 3 1	5647.76	10.58
13	72.810	1.2979	5936.32	5	4 2 0	5945.01	−8.68

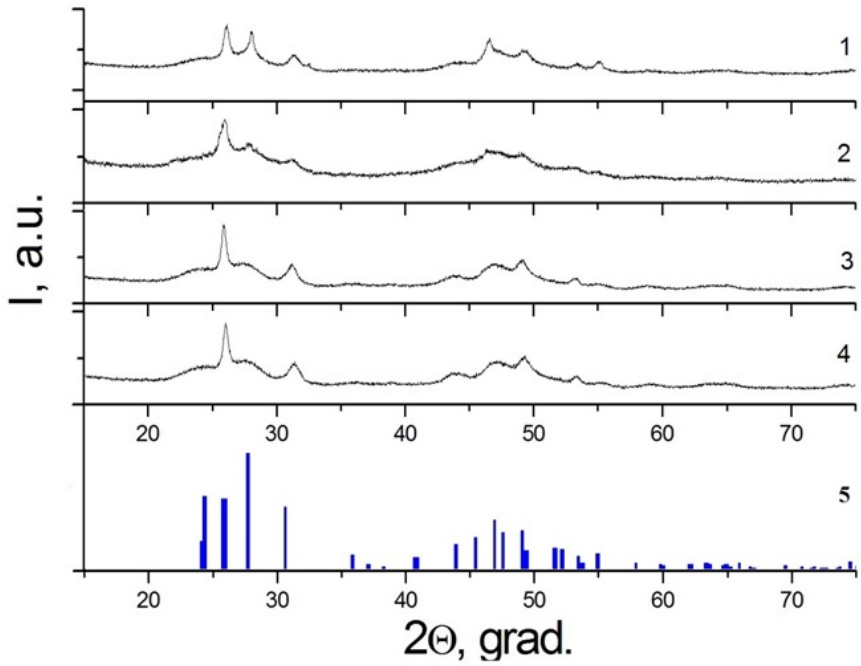

FIG. 5. X-Ray powder diffraction patterns for the specimens obtained by co-precipitation of calcium and yttrium fluorides from aqueous nitrate solutions (second set of experiments): 80 mol.% (1), 85 mol. % (2), 90 mol. % (3), 95 mol.% (4), and JCPDS Card No. 74-0911 for β-YF_3 phase (5)

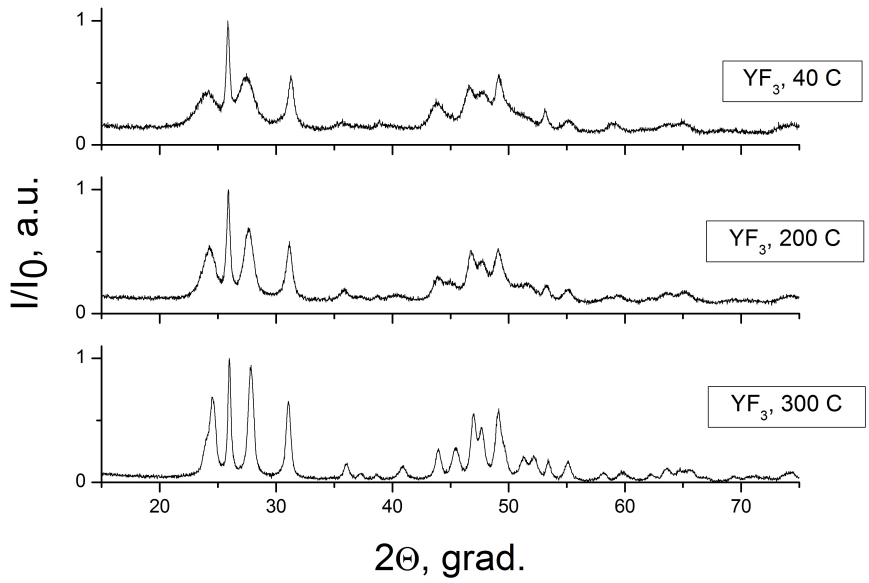

FIG. 6. X-Ray powder diffraction patterns for the YF_3 specimens: freshly prepared, $a = 6.294(3)$, $b = 6.867(4)$, $c = 4.528(3)$ Å (1), annealed at 200 °C, $a = 6.317(2)$, $b = 6.875(2)$, $c = 4.469(2)$ Å (2), YF_3 annealed at 300 °C, $a = 6.346(1)$, $b = 6.861(1)$, $c = 4.419(1)$ Å (3)

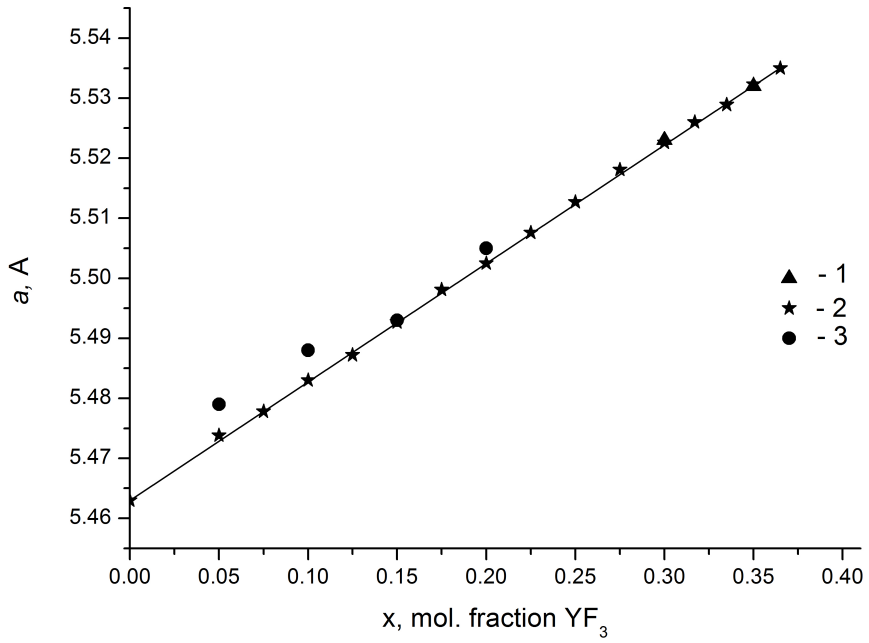

FIG. 7. Unit cell parameters for $Ca_{1-x}Y_xF_{2+x}$ fluorite-type solid solutions as per Fedorov et al. [7] (1) and Gettmann and Greis [12] (2), (all specimens were synthesized by solid phase synthesis) along with the present work data for $Ca_{1-x}Y_xF_{2+x}$ nanopowders (3). Straight-line dependence according to Fedorov and Sobolev [55]

have come from 8 wt. % loss from decomposition:

$$(H_3O)Y_3F_{10} \rightarrow 3YF_3 + H_2O + HF \tag{2}$$

along with additional evaporation of hydration water from the solid sample.

Structure of KY_3F_{10} type is derived from fluorite. It consists of a 3D framework formed by $(Y_6F_{35})^{18-}$ clusters (Fig. 2) interconnected by their vertices. Monovalent cations occupy cavities of the aforementioned framework [14, 55, 56]. KR_3F_{10} (R = Dy–Lu, Y) and RbR_3F_{10} (R = Sm–Tb) [3] crystallize in this structure type. However, the structure for KY_3F_{10} can also can be described as a 3D framework of $(Y_6F_{32})^{14-}$ clusters (constructed from Thompson antiprism coordination yttrium polyhedra in another way) [57] that are also present in the structure of $(H_3O)Y_3F_{10}nH_2O$ phase (*Fd3m* SSG, Z = 16) [36]. However, the latter clusters are packed in a different manner, and the previously described $(H_3O)Y_3F_{10}nH_2O$ phase (*Fd3m* SSG, Z = 16) is not a fluorite-type phase, in contrast with the phase obtained in our experiments for 90 % YF_3-10% CaF_2 solid solution specimen (Table 2).

The above results for the CaF_2–YF_3 system, obtained by co-precipitation method, are similar to our data for the CaF_2–HoF_3 system [54]. They are also in a good agreement with data [43] regarding $Ca_{1-x}R_xF_{2+x}$ solid solutions. Weak additional lines in the X-ray diffraction patterns, corresponding to β-YF_3 nanoparticles, were also observed for $Ca_{0.6}Y_{0.4}F_{2.4}$, also synthesized by the aforementioned co-precipitation in [45].

It is also worth mentioning that we did not observe the formation of tysonite-type phase(s) in the co-precipitated specimens at the lower temperatures. This should not be surprising if one takes into account that such a tysonite-type phase is stable at higher temperatures only (Fig. 1). Nevertheless, it is quite strange that there was no fluorite-type solid solutions formed in the CaF_2-RF_3 systems (R = rare earth element) that contain a relatively high concentration of the rare earth metals (35–40 mol. % RF_3) and possess ordered fluorite-type structures (such ordered phases are usually thermodynamically stable at the lower temperatures). The other previously studied MF_2–RF_3 systems (e.g., SrF_2–YF_3 [53], BaF_2–YF_3 [49], BaF_2–CeF_3 [52]) with M = Sr and Ba have exhibited different features: each of these systems had the concentration ranges, where ordered fluorite-type phases were observed under equilibrium conditions at the higher temperatures, the unordered solid solutions were formed. Currently, it is hard to find a reasonable explanation for the different results for calcium fluoride systems.

In conclusion, results of our study demonstrate that in the course of the synthesis of $Ca_{1-x}Y_xF_{2+x}$ solid solutions by co-precipitation from aqueous media, the single phase specimens have been formed for the relatively low yttrium content only (up to 20 mol. % YF_3). These samples, apparently, are not under equilibrium, but they

are fairly stable and do not undergo any detectable changes over the course of a few years. The latter is crucially important for the preparation of materials of practical value [58].

Acknowledgments

The authors express their appreciation to R. Ermakov for his kind assistance in the X-ray diffraction experiments as well as to V. K. Ivanov for his valuable discussion of the obtained results. The authors also wish to thank E. V. Chernova and A. I. Popov for their help in the preparation of the present manuscript.

This work was partially supported by RFBR 15-08-02481-a grant.

References

[1] Thoma R.E., Hebert G.M., Insley H., Weavwe C.F. Phase equilibria in the system sodium fluoride-yttrium fluoride. *Inorg. Chem.*, 1963, **2**(5), P. 1005–1012.

[2] Fedorov P.P., Sobolev B.P., Belov S.F. Fusibility diagram of the system NaF-YF_3, and the cross-section $Na_{0.4}Y_{0.6}F_{2.2}$-YOF *Inorg. Mater.*, 1979, **15**(5), P. 640–643.

[3] Fedorov P.P. Systems of alcali and rare-earth metal fluorides. *Russian J. Inorg. Chem.*, 1999, **44**(11), P. 1703–1727.

[4] Fedorov P.P., Kuznetsov S.V., Osiko V.V. Elaboration of nanofluorides and ceramics for optical and laser applications. Chapter in the book *Photonic & Electronic Properties of Fluoride Materials*, Ed. Tressaud A., Poeppelmeier K., Amsterdam et al.: Elsevier, 2016, P. 7–31.

[5] Fedorov P.P. Heterovalent isomorphism and solid solutions with a variable number of ions in the unit cell. *Russ. J. Inorg. Chem.*, 2000, **45**, Suppl. 3, P. S268–S291.

[6] Vogt T. Uber die Flusspat-Yttrofluoritgruppe. *Neues Jahrb. Mineral*, 1914, **2**(1), P. 9–13.

[7] Fedorov P.P., Izotova O.E., Alexandrov V.B., Sobolev B.P. New phases with fluorite-derived structure in CaF_2 - (Y, Ln)F_3 systems. *J. Solid State Chem.*, 1974, **9**(4), P. 368–374.

[8] Seiranian K.B., Fedorov P.P., Garashina L.S., Molev G.V., Karelin V.V., Sobolev B.P. Phase diagram of the system CaF_2 -YF_3. *J. Crystal Growth*, 1974, **26**(1), P. 61–64.

[9] *Crystals with the fluorite structure*. Ed. Hayes W. Oxford: Clarendon Press, 1974, 448 pp.

[10] Fedorov P.P., Sobolev B.P. Variable-composition phases with the LaF_3 structure in the systems MF_2-(Y,Ln)F_3. II. The systems CaF_2-(Y,Ln)F_3 (thermal characteristics and formation of berthollides). *Kristallografiya*, 1975, **20**(5), P. 584–586.

[11] Sobolev B.P., Aleksandrov V.B., Fedorov P.P., et al. Variable-composition phases with the LaF_3 structure in the systems MF_2-(Y,Ln)F_3. IV. X-ray characteristics, heterovalent isomorphic substitutions. *Kristallografiya*, 1976, **21**(1), P. 49–54.

[12] Gettmann W., Greis O. Uber fluorit- und tysonitverwandte Ordnungsphasen im System CaF_2-YF_3. *J. Solid State Chem.*, 1978, **26**(2), P. 255–263.

[13] Kaminskii A.A. *Laser crystals: their physics and properties*. Berlin, Heidelberg: Springer Verlag, 1990, 459 pp.

[14] Greis O., Hashke J.M. Rare earth fluorides. In *Handbook on the Physics and Chemistry of Rare Earth*. Amsterdam: Elsevier, 1982, v.**5**, P. 387–460.

[15] Kuntz A.F. Fluorite crystallization under hydrothermal conditions. *Proc. of Geology Institute, Komi department of USSR Academy of Sciences*, 1982, **39**, P. 31–41. (in Russian)

[16] Otroshchenko L.P., Aleksandrov V.B., Bydanov N.N., Simonov V.I., Sobolev B.P. Neutron-diffraction structure refinement of the $Ca_{0.90}Y_{0.10}F_{2.10}$ solid solution. *Kristallografiya*, 1988, **33**(3), P. 764–765. (in Russian)

[17] Ivanov-Shits A.K., Sorokin N.I., Fedorov P.P., Sobolev B.P. Specific features of ionic transport in nonstoichiometric fluorite-type $Ca_{1-x}R_xF_{2+x}$ (R = La-Lu, Y, Sc) phases. *Solid State Ionics*, 1990, **37**, P. 125–137.

[18] Sobolev B.P. *The rare earth trifluorides. Part 1. The high temperature chemistry of the rare earth trifluorides*. Barcelona: Institut d'Estudis Catalans, 2000, 520 pp.

[19] Sobolev B.P. *The rare earth trifluorides. Part 2. Introduction to materials sience of multicomponent metal fluoride crystals.* Barcelona: Institut d'Estudis Catalans, 2001, 459 pp.

[20] Karimov D.N., Krivandina E.A., Zhmurova Z.I., Sobolev B.P., Bezhanov V.A., Chernov S.P., Shapochkin G.M. Investigation of multicomponent fluoride optical materials in the UV spectral region: I. Single crystals of $Ca_{1-x}R_xF_{2+x}$ (R = Sc, Y, La, Yb, Lu) solid solutions. *Crystallogr. Rep.*, 2006, **51**(6), P. 1009–1015.

[21] Fedorov P.P. Third law of thermodynamics as applied to phase diagrams. *Russ. J. Inorg. Chem.*, 2010, **55**(11), P. 1722–1739.

[22] Bolotina N.B., Kalyukanov A.I., Chernaya T.S., Verin I.A., Buchinskaya I.I., Sorokin N.I., Sobolev B.P. X-ray and neutron diffraction study of the defect crystal structure of the as-grown nonstoichiometric phase $Y_{0.715}Ca_{0.285}F_{2.715}$. *Crystallogr. Rep.*, 2013, **58**(4), P. 575–585.

[23] Popov P.A., Fedorov P.P., Osiko V.V. Thermal conductivity of single crystals of the $Ca_{1-x}Y_xF_{2+x}$ solid solution. *Doklady Physics*, 2014, **59**(5), P. 199–202.

[24] Krahl T., Scholz G., Kemnitz E. Solid Solutions CaF_2-YF_3 with fluorite structure prepared on the solgel route: investigation by multinuclear MAS NMR spectroscopy. *J. Phys. Chem. C*, 2014, **118**, P. 21066–21074.

[25] Bergstol S., Jensen B.B., Neuman H. Tveitite, a new calcium yttrium fluoride. *Lithos*, 1977, **10**, P. 81–87.

[26] Bevan D.J.M., Strahle J., Greis O. The crystal structure of tveitite, an ordered yttrofluorite mineral. *J. Solid State Chem.*, 1982, **44**, P. 75–81.

[27] Atencio D., Bastos Neto A.C., Pereira V.P., et al. Waimirite-(Y), orthorhombic YF_3, a new mineral from the Pitinga mine, Presidente Figueiredo, Amazonas, Brazil and from Jabal Tawlah, Saudi Arabia: description and crystal structure. *Mineral. Magazine*, 2015, **79**(3), P. 767–780.

[28] Fedorov P.P. Association of point defects in non stoichiometric $M_{1-x}R_xF_{2+x}$ fluorite-type solid solutions. *Butll. Soc. Cat. Cien.*, 1991, **12**(2), P. 349–381.

[29] Kazanskii S.A., Ryskin A.I., Nikiforov A.E., Zaharov A.Yu., Ougrumov M.Yu., Shakurov G.S. EPR spectra and crystal fleld of hexamer rare-earth clasters in fluorites. *Phys. Rev. B*, 2005, **72**, 014127 P. 1–11.

[30] Popov P.A., Dykel'skii K.V., Mironov I.A., Demidenko V.A., Smirnov A.N., Smolyanskii P.L., Fedorov P.P., Osiko V.V., Basiev T.T.. Thermal conductivity of CaF_2 optical ceramics. *Doklady Physics*, 2007, **52**(1), P. 7–9.

[31] Turkina T.M., Fedorov P.P., Sobolev B.P. Stability of plane crystallization front in growth of single crystals of solid solutions $M_{1-x}R_xF_{2+x}$ (where M = Ca,Sr,Ba, R = rare earth) from a melt *Kristallografiya*, 1986, **31**(1), P. 83–87.

[32] Kuznetsov S.V., Fedorov P.P. Morphological Stability of Solid-Liquid Interface during Melt Crystallization of Solid Solutions $M_{1-x}R_xF_{2+x}$. *Inorg. Mater.*, 2008, **44**(13), P. 1434–1458. (Supplement)

[33] Sobolev B.P., Fedorov P.P. Hexagonal YF_3' structure type and high-temperature modifications of rare-earth trifluorides isostructural with YF_3. *Kristallografiya*, 1973, **18**(3), P. 392.

[34] Kuznetzov S.V., Osiko V.V., Tkatchenko E.A., Fedorov P.P. Inorganic nanofluorides and related nanocomposites. *Russian Chem. Rev.*, 2006, **75**(12), P. 1065–1082.

[35] Fedorov P.P., Luginina A.A., Kuznetsov S.V., Osiko V.V. Nanofluorides. *J. Fluorine Chem.*, 2011, **132**(12), P. 1012–1039.

[36] Lucier B.E.G., Johnston K.E., Arnold D.C., et. al. Comprehensive Solid-State Cheracterization of Rare Earth Fluoride Nanoparticles. *J. Phys. Chem. C*, 2014, **118**(2), P. 1213–1228.

[37] Van Veggel F.C.J.M. Upconversion of Ln^{3+}-based Nanoparticles for Optical Bio-imaging. In: *Luminescence of Lanthanide Ions in Coordination Compounds and Nanomaterials*. John Wiley Sons, 2014, P. 269–302.

[38] Fedorov P.P., Luginina A.A., Popov A.I. Transparent Oxyfluoride Glass Ceramics. *J. Fluorine Chem.*, 2015, **172**, P. 22–50.

[39] Naccache R., Yu Q., Capobianco J.A. The fluoride host: nucleation, growth, and upconversion of lanthanide-doped nanoparticles. *Adv. Optical Mater.*, 2015, **3**(4), P. 482–509.

[40] Düvel A., Bednarcik J., Šepelák V., Heitjans P. Mechanosynthesis of the fast fluoride ion conductor $Ba_{1-x}La_xF_{2+x}$: from the fluorite to the tysonite structure. *J. Phys. Chem. C*, 2014, **118**, P. 7117–7129.

[41] G. Scholz, S. Breitfeld, T. Krahl, A. Düvel, P. Heitjans, E. Kemnitz. *Solid State Sciences*, 2015, **50**, P. 32–41.

[42] Lei Lei, Daqin Chen, Feng Huang , Yunlong Yu, Yuansheng Wang. *J. Alloys Comp.*, 2012, **540**, P. 27–31.

[43] Kouznetzov S.V., Yarotskya I.V., Fedorov P.P., Voronov V.V., Lavristchev S.V., Basiev T.T., Osiko V.V. Preparation of Nanopowdered $M_{1-x}R_xF_{2+x}$ (M = Ca, Sr, Ba; R = Ce, Nd, Er, Yb) Solid Solutions. *Russian J. Inorg. Chem.*, 2007, **52**, P. 315–320.

[44] Fedorov P.P., Kuznetsov S.V., Voronov V.V., Yarotskya I.V., Arbenina V.V. Soft chemical synthesis of $NaYF_4$ nanopowders. *Russian J. Inorg. Chem.*, 2008, **53**(11), P. 1681–1685.

[45] Fedorov P.P., Kuznetsov S.V., Mayakova M.N., et al. Coprecipitation from aqueous solutions to prepare binary fluorides. *Russian J. Inorg. Chem.*, 2011, **56**(10), P. 1525–1531.

[46] Luginina, A.A., Fedorov, P.P., Kuznetsov, S.V., et al., Synthesis of ultrafine fluorite $Sr_{1-x}Nd_xF_{2+x}$ powders. *Inorg. Mater.*, 2012, **48**(5), P. 531–538.

[47] Kuznetsov, S.V., Ovsyannikova, A.A., Tupitsyna, E.A., Yasyrkina, D.S., Voronov, V.V., Fedorov, P.P., Batyrev, N.I., Iskhakova, L.D., Osiko, V.V. Phase formation in LaF_3-$NaGdF_4$, $NaGdF_4$-$NaLuF_4$, $NaYF_4$-$NaLuF_4$ systems: synthesis of powders by co-precipitation from aqueous solutions. *J. Fluor. Chem.*, 2014, **161**, P. 95–101.

[48] S.V. Kuznetsov, D.S. Yasyrkina, A.V. Ryabova, D.V. Pominova, V.V. Voronov, A.E. Baranchikov, V.K. Ivanov, P.P. Fedorov. α-$NaYF_4$:Yb:Er@AlPc$(C_2O_3)_4$ -Based efficient up-conversion luminophores capable to generate singlet oxygen under IR excitation. *J. Fluor. Chem.*, 2016, **182**, P. 104–108.

[49] Fedorov P.P., Mayakova M.N., Kuznetsov S.V., Voronov V.V., Ermakov R.P., Samarina K.S., Popov A.I., Osiko V.V. Co-Precipitation of yttrium and barium fluorides from aqueous solutions. *Mat. Res. Bull.*, 2012, **47**, P. 1794–1799.

[50] Fedorov P.P., Mayakova M.N., Kuznetsov S.V., Voronov V.V., Osiko V.V., Ermakov R.P., Gontar' I.V., Timofeev A.A., Iskhakova L.D. Coprecipitation of barium–bismuth fluorides from aqueous solutions: nanochemical effects. *Nanotechnologies in Russia*, 2011, **6**, P. 203–210.

[51] Mayakova M.N., Kuznetsov S.V., Voronov V.V., Baranchikov A.E., Ivanov V.K., Fedorov P.P. Soft chemistry synthesis of powders in the BaF_2-ScF_3 system. *Russian J. Inorg. Chem.*, 2014, **59**(7), P. 773–777.

[52] Mayakova M.N., Voronov V.V., Iskhakova L.D., Kuznetsov S.V., Fedorov P.P. Low-temperature phase formation in the BaF_2-CeF_3 system. *J. Fluorine Chem.*, 2016, **187**, P. 33–39.

[53] Mayakova M.N., Luginina A.A., Kuznetsov S.V., Voronov V.V., Ermakov R.P., Baranchikov A.E., Ivanov V.K., Karban' O.V., Fedorov P.P. Synthesis of SrF_2-YF_3 nanopowders by co-precipitation from aqueous solutions. *Mendeleev Communications*, 2014, **24**(6), P. 360–362.

[54] Fedorov P.P., Mayakova M.N., Kuznetsov S.V., Voronov V.V. Low temperature phase formation in the CaF_2 - HoF_3 system. *Russian J. Inorg. Chem.*, 2017, **62**(9), P. 1173–1176.

[55] Fedorov P.P., Sobolev B.P. Concentration dependence of unit-cell parameters of phases $M_{1-x}R_xF_{2+x}$ with the fluorite structure. *Sov. Phys. Crystallogr*, 1992, **37**(5), P. 651–656.

[56] Ayala F.P., Oliveira M.A.S., Gesland J.-Y., Moreira R.L. Electrical and dielectrical investigation of the conduction processes in KY_3F_{10} crystals. *J. Phys. C.: Condensed Matter*, 1998, **10**, P. 5161–5170.

[57] Podberezskay N.V., Potapova O.G., Borisov S.V., Gatilov Yu. V. KTb_3F_{10}crystal structure – cubic pacing of $[Tb_6F_{32}]^{14-}$ polyanions. *J. Struct. Chem.*, 1976, **17**(5), P. 948–950. (in Russian)

[58] Vahrenev R.G., Mayakova M.N., Kuznetsov S.V., Ryabova A.V., Pominova D.V., Voronov V.V., Fedorov P.P. The research of synthesis and luminescent characteristics of calcium fluoride doped with ytterbium and erbium for biomedical application. *Condensed Media and Interface Borders*, 2016, **18**(4), P. 478–484.